High Density Labeling of Polymerase Chain Reaction Products with the Fluorescent Base Analogue tCo

ARTICLE *in* ANALYTICAL CHEMISTRY · OCTOBER 2009

Impact Factor: 5.64 · DOI: 10.1021/ac9017555 · Source: PubMed

4 AUTHORS, INCLUDING:

Milan Urban
Palacký University of Olomouc
33 PUBLICATIONS **690** CITATIONS
SEE PROFILE

Robert Kuchta
University of Colorado Boulder
91 PUBLICATIONS **2,672** CITATIONS
SEE PROFILE

Published in final edited form as:
Anal Chem. 2009 November 1; 81(21): 9079–9085. doi:10.1021/ac9017555.

High Density Labeling of PCR Products with the Fluorescent Analogue tCo

Gudrun Stengel,
Department of Chemistry and Biochemistry, University of Colorado, Boulder, CO 30309-0215

Milan Urban,
Department of Chemistry and Biochemistry, University of Colorado, Boulder, CO 30309-0215

Byron W. Purse, and
Department of Chemistry and Biochemistry, University of Denver, Denver, Colorado 80208

Robert D. Kuchta*
Department of Chemistry and Biochemistry, University of Colorado, Boulder, CO 30309-0215

Abstract

Fluorescent DNA of high molecular weight is an important tool for studying the physical properties of DNA and DNA-protein interactions and it plays a key role in modern biotechnology for DNA sequencing and detection. While several DNA polymerases can incorporate large numbers of dye-linked nucleotides into primed DNA templates, the amplification of the resulting densely labeled DNA strands by PCR is problematic. Here, we report a method for high density labeling of DNA in PCR reactions employing the 5'-triphosphate of 1, 3-diaza-2-oxo-phenoxazine (tCo) and Deep Vent DNA polymerase. tCo is a fluorescent cytosine analogue that absorbs and emits light at 365 and 460 nm, respectively. We obtained PCR products that were fluorescent enough to directly visualize them in a gel by excitation with long UV light, thus eliminating the need for staining with ethidium bromide. Reactions with Taq polymerase failed to produce PCR products in the presence of only small amounts of dtCoTP. A comparative kinetic study of Taq and Deep Vent polymerase revealed that Taq polymerase, although it inserts dtCoTP with high efficiency opposite G, is prone to forming mutagenic tCo-A base pairs and does not efficiently extend base pairs containing tCo. These kinetics features explain the poor outcome of the PCR reactions with Taq polymerase. Since tCo substitutes structurally for cytosine, the presented labeling method is believed to be less invasive than labeling with dye-linked nucleotides and therefore produces DNA that is ideally suited for biophysical studies.

Keywords

Taq; Deep Vent; DNA polymerase; kinetics; dNTP

Many methods in molecular biology rely on fluorescently labeling DNA. Classical applications include the visualization of PCR products, the analysis of base mutations (1), transcription and gene expression (2), in situ hybridization (3) and four-color DNA sequencing (4,5). Fluorescent probes constitute far more than an environmentally friendly alternative to radioactive markers; they offer a range of physical properties that have inspired novel technologies for DNA analysis. For instance, real-time PCR probes have been designed based on the possibility of switching between bright and dark states in response to distance dependent fluorescent quenching (6–9) or to intercalation of dyes into duplex DNA (10,11). Methods for the detection

* To whom correspondence should be addressed. kuchta@colorado.edu. Phone: 303-492-7027. Fax: 303-492-5894.

of single nucleotide polymorphisms exploit the spectral sensitivity of some fluorescent probes to a specific base context (12–16). The most notable recent invention is probably the introduction of single-molecule DNA sequencing schemes, which are expected to revolutionize the pace of genomic research. Single molecule sequencing critically depends on completely replacing one or all four nucleobases by a fluorescent reporter to create a color-coded DNA sequence (17–20).

While solid phase DNA synthesis has made internal and terminal labeling of short (100–200 bases long) oligonucleotides straightforward (21), a fully synthetic route for high-density labeling of large DNA fragments is not yet available. Instead, one depends on the sequence specific incorporation of reporter nucleotides by DNA polymerases (DNA pol [1]) (22–24). In principle, there are three different choices of reporters; (i) a nucleotide analogue that exhibits a functional group that can be rendered fluorescent in a post-synthetic reaction (25,26), for instance by covalent attachment of a dye, a digoxigenin-coupled enzyme reaction or by affinity labeling.(27); (ii) a dye-linked nucleotide consisting of a conventional dye attached to the canonical base via a carbon linker, and; (iii) a fluorescent base analogue (22–24,28,29). These base analogues are usually designed to closely resemble naturally occurring bases, but their structure exhibits small modifications that render them fluorescent. To label DNA with fluorescent nucleotide analogues instead of using dye-linked nucleotides entails the significant advantage of placing the dye at a defined position inside the DNA helix (30). Thus, the hydrodynamic radius of the DNA remains unchanged and the outer sphere of the DNA is not rendered hydrophobic by dyes protruding from the helix.

The systematic evaluation of the ability of different DNA pols to insert dye-linked nucleotides into DNA revealed several trends. First, B family DNA pols (e.g. Vent pol) tend to incorporate dye-linked nucleotides with higher efficiency than A family enzymes (e. g. Taq pol), in some cases even allowing for the complete substitution of a canonical base by its fluorescent counterpart.(22,24) Second, increasing the length of the carbon tether that spatially separates the dye from the DNA increases the efficiency of incorporation (3). Third, dye-linked bases are subjected to exonuclease digestion, requiring the use of exonuclease-deficient DNA polymerases. And fourth, depending on the hydrophobicity of the dye, multi-labeling can render DNA insoluble, leading to precipitation (24).

In the aforementioned studies, the dye-linked nucleotides were primarily tested as substrates in primer extension assays, i.e. the resulting DNA is only labeled in the primer strand and no amplification of the starting DNA was achieved. Here, we describe a method for the labeling of PCR fragments with the fluorescent nucleotide analogue 1, 3-diaza-2-oxo-phenoxazine (tCo, Figure 1). tCo is a structural analogue of cytosine that is expanded by two aromatic rings in the direction of the major groove but has full hydrogen bonding capability with guanine and base stacks tightly with the duplex when inserted opposite G.(31–33) tCo maximally absorbs at 365 nm and the compound emits light at 460 nm with the fluorescence quantum yield ranging between 0.2–0.3, depending on the neighboring bases.(34) Recently, we showed that several A and B family DNA pols efficiently substitute tCo for cytosine and continue adding dNTPs (35,36). Using dtCoTP and exonuclease-deficient Deep Vent pol, we have developed a PCR method to produce large, highly fluorescent DNA fragments that can be directly visualized in gels based on their tCo fluorescence emission and without staining. Additionally, we present kinetic studiues comparing the ability of Taq pol and Deep Vent pol to process tCo, and we briefly discuss fluorescence quenching mechanisms that are active in multi-tCo labeled DNA.

[1]Abbreviations used: DNA pol, DNA polymerase; dtCoTP, 1,3-diaza-2-oxo-phenoxazine-2'-deoxyribose-5'-triphosphate; Taq pol, *Thermus aquaticus* DNA polymerase; Deep Vent pol, DNA polymerase from *Pyrococcus species* GB-D; Tris-HCl, Tris(hydroxymethyl) aminomethane, HCl salt; EDTA, ethylene diamine tetraacetic acid; TAE, Tris-acetate-EDTA; EtBr, ethidium bromide; QY, fluorescence quantum yield

Experimental Section

Materials and Enzymes

Unlabeled dNTPs were from Invitrogen and ^{32}P-labeled NTPs from Perkin Elmer Life Sciences. The 1,3-diaza-2-oxo-phenoxazine nucleoside was synthesized according to Matteucci et al. (32) and converted into the 5'-triphosphate following the procedure by Ludwig (37). The concentration of dtCoTP was determined based on the absorption of tCo at 260 nm (ε_{tCo} = 11,000 M^{-1} cm^{-1}). Taq DNA pol was purchased from Invitrogen, Deep Vent exo- pol and DNase I were from New England Biolabs, and exonuclease I was from USB Affimetrix. Synthetic oligonucleotides were synthesized by Integrated DNA Technology and the plasmid coding for the globin protein was a generous gift from Jens Lyke-Andersen (University of Colorado Boulder).

PCR reactions and analysis

The 560 bp DNA fragment coding for the beta chain of human hemoglobin was amplified using 5'GTACGGTGGGAGGTCTATAT 3' (forward primer) and5'ACCACTTTCTGATAGGCAGC 3' (reverse primer). The reactions (50 μL) contained the buffers and Mg^{2+} concentrations recommended by the suppliers of the DNA polymerases. For Deep Vent exopol: 10 mM KCl, 10 mM $(NH_4)_2SO_4$, 20 mM Tris-HCl pH 8.8, 2 mM $MgSO_4$, 0.1 % Triton X-100. For Taq pol: 20 mM Tris-HCl pH 8.4, 50 mM KCl, 1.5 mM $MgCl_2$. In addition, the reactions contained 200 μM of each dNTP, 500 nM forward and reverse primer, 140 ng template and either 1 unit Deep Vent pol or 2.5 units Taq pol. The sum of dtCoTP and dCTP concentration always equaled 200 μM. The standard temperature protocol for reactions containing 15 % glycerol was: Step 1: 94 °C/4 min; step 2: 95 °C/45 sec; step 3: 52 °C/30 sec; step 4: 73 °C/2 min; step 5: 99 °C/45 sec; step 6: 55 °C/30 sec; step 7: 73 °C/2 min; go to step 5: 40-times; final elongation: 73 °C/20 min. The lower annealing temperature (step 3) was used in the first cycle to account for the lower melting temperature of tCo-free DNA. The reactions were performed using an Eppendorf Mastercycler. The PCR reactions were analyzed using 1.2 % agarose gels with 0.5 × TAE buffer. The gels were either exposed at 365 nm or at 254 nm after staining of the DNA bands with ethidium bromide.

Analysis of PCR products by native gel electrophoresis

To monitor the increase in molecular mass of the PCR products due to incorporation of increasing dtCoTP concentrations, we repeated the PCR reactions using [^{32}P]-labeled forward and reverse primers. Aliquots of the PCR reactions were mixed with 6x gel loading buffer (40 % sucrose) and electrophoresed on a 7 % polyacrylamide, 1x TBE gel. The gel was dried and the DNA bands visualized by phosphor imaging.

Enzymatic digest of PCR products

10 μL of each PCR reaction were analyzed on a 1.2 % agarose gel, the DNA bands were visualized by long UV excitation and the bands of interest excised. The excised DNA bands were subsequently worked up using a QiaQuick gel extraction kit (Qiagen), resulting in 30 μL of DNA in 10 mM Tris-HCl pH 8. 10 μL of this solution were added to 110 μL of 10 mM Tris-HCl pH 7.6, 2.5 mM $MgCl_2$ and 0.5 mM $CaCl_2$. DNA degradation was initiated by addition of 1unit DNAse I and 10 units Exonuclease I at room temperature. Using a steady-state fluorimeter (Quantamaster from Photon Technology International), fluorescence emission spectra were recorded before and after DNA digestion using an excitation wavelength of 345 nm. To continuously measure the time courses of fluorescence dequenching the excitation wavelength was set to 345 nm, the emission to 460 nm.

Determination of kinetic parameters

5'-labeling of primer strands

DNA primers were 5'-^{32}P-labeled using T4 polynucleotide kinase (New England Biolab) and [γ-^{32}P]ATP. The labeled primer was gel-purified and annealed to the appropriate template strands.

Polymerization assays

All assays were conducted using 0.5 μM 5'- ^{32} P-primer/template and between 0.3 and 300 μM natural or analogue dNTP, depending on the particular assay. Four different primer/template sequences were used:

DNA_A	5'-TCCATATCACAT 3'-AGGTATAGTGTAACTCTTATCATCT
DNA_C	5'-TCCATATCACAT 3'-AGGTATAGTGTACTTCTTATCTATCT
DNA_G	5'-TCCATATCACAT 3'-AGGTATAGTGTAGCTCTTATCTATCT
DNA_{tCo}	5'-TCCATATCACAT 3'-AGGTATAGTGTA(tCo)ATCTTATCTATCT

The reaction buffers were 10 mM KCl, 10 mM $(NH_4)_2SO_4$, 20 mM Tris-HCl pH 8.8, 2 mM $MgSO_4$, 0.1 % Triton X-100 and 0.05 mg/ml bovine serum albumin for Deep Vent exo- pol, and 20 mM Tris-HCl pH 8.4, 50 mM KCl, 1.5 mM $MgCl_2$ and 0.05 mg/ml bovine serum albumin for Taq pol. The total reaction volume was either 5 or 10 μL. Polymerization was initiated by mixing equal volumes of reaction mixture and enzyme followed by incubation at 37 °C. The enzyme concentrations used for the determination of V_{max} and K_M were 0.0125 units/μL Taq pol and 0.0005 units/μL Deep Vent pol, respectively. Two volumes gel loading buffer (90 % formamide with 50 mM EDTA) were added to stop the reactions. The extension products were separated by denaturing gel electrophoresis (20 % polyacrylamide, 8 M urea) and analyzed by phosphor imaging (Typhoon scanner, Molecular Dynamics). The parameters V_{max} and K_M were obtained by plotting the amount of primer extension as a function of dNTP concentration and subsequent non-linear curve fitting of the data to the Michaelis-Menten equation (38).

Competitive single nucleotide extension assays

To measure the competitive insertion of dCTP and dtCoTP across from G, assays contained DNAG and in total 100 μM dNTP. The mixing ratio of dCTP and dtCoTP was varied in steps of 10 μM, i. e. 10 μM dCTP and 90 μM dtCoTP, 20 μM dCTP and 80 μM dtCoTP etc. Deep Vent pol was employed at a concentration of 0.001 units/μL, Taq pol at 0.05 units/μL and the reactions stopped after 5 and 10 minutes, respectively. After quantifying the fraction of primer that had been extended by tCo or by C, the relative kcat/K_M values were determined graphically using the following equation: $$\frac{1}{\text{fraction}_{dNTP}} = \frac{\left(\frac{kcat}{K_M}\right)_{dtCoTP}}{\left(\frac{kcat}{K_M}\right)_{dNTP}} \cdot \frac{[dtCoTP]}{[dCTP]}$$, with fraction dNTP being the amount of primer extended by C in this case. Analogous experiments were performed with DNAA and mixtures of dtCoTP and dTTP.

Read through assays

The reactions contained 0.5 μM of the designated [^{32}P]-primer/template, 25 μM of each dNTP and 0.0125 units/μL Taq pol or 0.0005 units/μL Deep Vent pol, respectively. 2 μL aliquots

were removed from the master mix after 5, 10, 20 and 30 min and quenched with two volumes of 90 % formamide with 50 mM EDTA. Analysis of the reaction products was conducted by denaturing gel electrophoresis as described above.

Results and Discussion

PCR reactions under optimized denaturation conditions

First, we compared the ability of Deep Vent exo- and Taq pol to produce a 560 base pair long PCR fragment in the presence of various mixing ratios of dtCoTP and dCTP. The gene we amplified codes for the beta chain of human hemoglobin and has a GC content of 53 %. The template was chosen arbitrarily without consideration of the exact base sequence. As described in detail in the experimental section, the reactions were largely performed under standard conditions, using 200 μM of each dNTP, with [dtCoTP] + [dCTP] = 200 μM in cases where dtCoTP substituted for dCTP. In our initial experiments, the PCR cycle included the standard denaturation step of 45 sec at 95°C. Figure 2 A and B show agarose gels of the PCR products obtained with Taq and Deep Vent pol as increasing amounts of dCTP were replaced by dtCoTP. Before staining of the gels with ethidium bromide, we exposed the gels on a 365 nm trans-illuminator to detect the tCo emission. At this wavelength, we were not able to see the DNA ladder or the positive control containing only 200 μM dCTP, however, the PCR products obtained in the presence of moderate to high dtCoTP concentrations were clearly visible. Reactions catalyzed by Taq pol did not result in PCR product for dtCoTP concentration > 10 μM, whereas Deep Vent pol tolerated dtCoTP concentrations up to 50 μM.

The failure of the PCR reactions at relatively low dtCoTP concentration did not agree with our previous kinetics study of the Klenow fragment, an A family polymerase like Taq, and human pol α, a B family polymerase like Deep Vent. Both pol α and Klenow fragment inserted dtCoTP with higher efficiency than dCTP and they could incorporate 4 consecutive tCo's with reasonable efficiency.(36) However, Sandin et al. showed that a single tCo-G base pair increases the melting temperature of a 10 base pair duplex on average by 3 °C (34). Thus, we reasoned that the accumulation of multiple tCo's in the DNA might stabilize it to an unusual degree. We therefore focused on the denaturation step as a possible cause for the outcome of the reactions. Indeed, when we repeated the reactions using a denaturation step at 99 °C for 45 sec, we obtained PCR products up to dtCoTP concentrations of 75–100 μM (Figure 2 C). While prolonging the denaturation step had no effect on the product distribution, we were able to further optimize the PCR reactions by adding 15 % glycerol, a molecule that lowers the melting temperature of DNA (Figure 2 D). The addition of other chemicals of this type, such as formamide and dimethylsulfoxide, had a similar effect on the yield of the reactions (data not shown).

We conclude that Deep Vent pol is capable of replacing at least 50 % of all C's with tCo, assuming dCTP and dtCoTP were incorporated with equal efficiency, and that the reactions are limited by the melting temperature of the resulting PCR product rather than by the substrate specificity of this pol over a wide range of dtCoTP concentrations. In the case of Taq pol however, we were not able to obtain PCR products using [dtCoTP] > 20 μM under any conditions. Thus, Deep Vent is clearly the superior polymerase for this application.

Variation of the number of amplification cycles

In theory, it is possible to obtain PCR product by only amplifying the original template but not the tCo modified amplification product (i.e,. linear PCR). The product yield would be low because every amplification cycle can only double the amount of starting template. However, conventional PCR can potentially double the total amount of DNA strands with every cycle, which causes the amount of amplification product to grow exponentially until the reaction

mixture is depleted of primer DNA, dNTPs or the polymerase loses activity. Depending on the amount of starting template, PCR reactions typically level off after 30 – 40 cycles. To explore if the dtCoTP containing PCR reactions match this exponential pattern we examined the amount of DNA product obtained after 10, 20, 30 and 40 cycles, using different mixing ratios of dtCoTP and dCTP (Figure 3). As expected, the amount of product increased dramatically between 10 and 20 cycles, whereas little or no change was observed between 30 and 40 cycles. Importantly, the dependence on the number of amplification cycles is similar for reactions with and without dtCoTP, suggesting that tCo-containing DNA is replicated with similar efficiency as unlabeled DNA.

Kinetic parameters for dtCoTP incorporation by Taq and Deep Vent pol and templating properties of tCo

Next we determined the kinetic parameters for the incorporation of dtCoTP and dCTP across from a template G by Taq and Deep Vent pol in competitive primer extension assays. Knowing the relative catalytic efficiencies would i) allow us to approximate the tCo labeling density of the PCR product at a given ratio of dtCoTP and dCTP and ii) possibly explain why Taq pol performs so much worse in the PCR reactions.

Deep Vent pol polymerizes dtCoTP 1.5-times more efficiently than dCTP (Table 1). Consequently, at the highest dtCoTP/dCTP ratio (5/3) that produces PCR product (Figure 2 D), around 71 % of the C's should be substituted by tCo (5×1.5/10.5 tCo + 3×1/10.5 C = 1). Taq pol prefers the nucleotide analogue even more, by a factor of 7.7. Theoretically, only 46 % of all C's are substituted by tCo at the highest dtCoTP/dCTP ratio (1/9) tolerated by Taq pol (1×7.7/16.7 tCo + 9×1/16.7 C = 1). Since the PCR reactions can tolerate a higher tCo content from the thermodynamic perspective, Taq pol must have other kinetic properties that interfere with the PCR.

We used synthetic primer/templates to determine if Taq and Deep Vent pol continue dNTP polymerization after inserting dtCoTP opposite G or dGTP opposite tCo, respectively (Figure 4, Table 3). In the presence of dtCoTP, dGTP, dATP and dTTP, Taq pol incorporates dtCoTP efficiently opposite G, but significant pausing occurs after incorporating the next nucleotide. By contrast Deep Vent pol reads through a tCo-G base pair without detectable pausing. A tCo in the template strand impairs both polymerases, however, the effects on Taq pol are much more severe. While Deep Vent pol forms the G-tCo base pair ~20-times less efficiently than a G-C pair, the difference is ~100-times for Taq pol (Table 2).

In total, the inferior performance of Taq pol is explained by the enzyme's preference for incorporating the nucleotide analogue, which is followed by subsequent pausing, paired with the inability to replicate tCo efficiently when encountered in the template.

Fluorescence quenching of tCo in duplex DNA

An interesting question relating to the design of the PCR experiments is if the highest tCo label density necessarily results in the most fluorescent PCR product. To find out if incorporation of large amounts of tCo into DNA results in self-quenching, we used a mixture of DNAse I and Exonuclease I to degrade the PCR products obtained at different dtCoTP/dCTP labeling ratios and monitored the fluorescence change after enzyme addition as a function of time (Figure 5 A). DNAse I nonspecifically cleaves DNA to release di, tri and longer oligonucleotides. Exonuclease I removes mononucleotides from single-stranded DNA in 3'-5' direction. Figure 5 A shows that substantial dequenching occurs as the DNA is broken down into nucleotides and that dequenching is more pronounced the higher the dtCoTP concentration in the PCR reaction. The final fluorescence intensity exceeds the starting value by a factor of 3.5 for PCR products generated in the presence of 75 μM dtCoTP, Dequenching is less

pronounced for the reaction with 100 μM dtCoTP. Since more dtCo should have been incorporated into DNA at this higher dtCoTP concentration, this result suggests that the enzymes are less efficient at digesting densely tCo labeled DNA.

What are the factors that account for the considerable extent of quenching? Sandin et al. measured the quantum yield of tCo in single and double-stranded DNA for all possible combination of adjacent 5' and 3' neighbors.(34) The quantum yield in the single strands varied between 0.14 and 0.40, yielding an average of 0.3, which in turn is equal to the quantum yield of the free nucleotide. However, the quantum yield likely depends on the base sequence of the entire oligonucleotide and possibly on its length. For instance, we measured a quantum yield of 0.3 for tCo flanked by two adenines in a DNA sequence unrelated to Sandin's study (Table 4, compare to quantum yield = 0.38 for 5'-…A(tCo)A in (34)). In duplex DNA, however, the quantum yield of tCo is 30–50 % lower than in the single strand.

Since no information regarding the quantum yield of multiple tCo's in DNA existed, we synthesized oligonucleotides containing 2 tCo's at four different separation distances (Table 4). The quantum yields of the tCo's varied in a non-systematical fashion between 0.25 and 0.3 in the single strand, and between 0.15 and 0.2 in the double strand. Thus, there is no obvious indication for long distance quenching via DNA-mediated electron transfer.(39) However, as expected for any dye, we observed very strong contact quenching when we examined a DNA strand with 4 consecutive tCo's. Here the quantum yield was only 0.03 (Table 4).

In summary, we ascribe intensity losses beyond 50 % primarily to collision quenching within tCo repeats and coiled secondary structures, without excluding the possibility of the existence of more cooperative phenomena that cannot be deduced by simple double labeling of short oligonucleotides. This quenching also suggests that the highest tCo label density will not necessarily result in the most fluorescent PCR product, particularly if there are large numbers of consecutive C's.

Possible mutagenic properties of tCo

Recently, we reported that Klenow and DNA pol α base-pair tCo almost ambivalently with G and A (36), whether tCo is located in the primer or in the template strand. We interpreted this observation as an indication for the existence of the imino tautomer of tCo, since this form is isosteric to T and as such would be capable of forming a Watson-Crick base pair with A. Consistent with these results both thermophilic pols show a trend for misinserting dtCoTP across a template A (Table 1). Deep Vent polymerizes dTTP 10-times more efficiently than dtCoTP across from A, whereas Taq pol prefers dTTP only by a factor of 3 (Table 1). Although the dTTP concentration is kept constant at 200 μM in all PCR reactions, the formation of tCo-A base pairs is a serious risk at high dtCoTP concentrations. For instance, at a dtCoTP/dTTP ratio of 1/2, around 5 % of all T-A base pairs would be mutated to tCo-A base pairs, which is equivalent to ~7 errors in a 560 nt single strand. If the resulting base mispairs are not readily extended, it would further explain why the PCR reactions fail at high dtCoTP concentration. Similarly, Deep Vent and Taq pol both prefer to insert dGTP over dATP, opposite a templating tCo by only a factor of around 25 (Table 2), which is too low a discrimination to exclude the formation of A-tCo base pairs at high dtCoTP concentration.

Conclusions

We have presented a method for the incorporation of the fluorescent nucleotide analogue dtCoTP into large DNA fragments by means of PCR. The PCR reactions rely on the use of an extremely thermostable B family DNA polymerase, Deep Vent exo-, which allows conducting the PCR reactions with a denaturation step at 99 °C without loss of enzyme activity. The resulting DNA fragments are highly fluorescent and can be visualized in a gel by excitation at

365 nm, thus obviating the need for staining of the DNA bands with carcinogenic DNA intercalating dyes such as ethidium bromide. Furthermore, unlike previously reported methods that use standard dNTPs containing covalently linked dyes to generate fluorescent DNA, using dtCoTP does not require the separation of unincorporated dNTP-fluorophore (24). Additionally, the presented labeling method is expected to have low impact on DNA solubility, on the mechanical properties of DNA in terms of bending, coiling and viscosity and on the ability of proteins to interact with DNA site-specifically or by linear diffusion along the DNA duplex.

Acknowledgments

This work was supported by NIH grants GM54194 and AI59764.

References

1. Syvanen AC. Nat Rev Genet 2001;2:930–942. [PubMed: 11733746]
2. Do JH, Choi DK. Eng Life Sci 2007;7:26–34.
3. Randolph JB, Waggoner AS. Nucleic Acids Res 1997;25:2923–2929. [PubMed: 9207044]
4. Chan EY. Mutat Res 2005;573:13–40. [PubMed: 15829235]
5. Kaiser RJ, Mackellar SL, Vinayak RS, Sanders JZ, Saavedra RA, Hood LE. Nucleic Acids Res 1989;17:6087–6102. [PubMed: 2771640]
6. Whitcombe D, Theaker J, Guy SP, Brown T, Little S. Nat Biotechnol 1999;17:804–807. [PubMed: 10429248]
7. Thelwell N, Millington S, Solinas A, Booth J, Brown T. Nucleic Acids Res 2000;28:3752–3761. [PubMed: 11000267]
8. Nazarenko IA, Bhatnagar SK, Hohman RJ. Nucleic Acids Res 1997;25:2516–2521. [PubMed: 9171107]
9. Holland PM, Abramson RD, Watson R, Gelfand DH. Proc Natl Acad Sci U S A 1991;88:7276–7280. [PubMed: 1871133]
10. Wittwer CT, Herrmann MG, Moss AA, Rasmussen RP. Biotechniques 1997;22:130–131. [PubMed: 8994660]
11. Higuchi R, Fockler C, Dollinger G, Watson R. Biotechnology 1993;11:1026–1030. [PubMed: 7764001]
12. Renard BL, Lartia R, Asseline U. Org Biomol Chem 2008;6:4413–4425. [PubMed: 19005602]
13. Wojciechowski F, Hudson RHE. J Am Chem Soc 2008;130:12574–12575. [PubMed: 18761442]
14. Cekan P, Sigurdsson ST. Chem Commun 2008:3393–3395.
15. Srivatsan SG, Weizman H, Tor Y. Org Biomol Chem 2008;6:1334–1338. [PubMed: 18385838]
16. Okamoto A, Saito Y, Saito I. Journal of Photochemistry and Photobiology C-Photochemistry Reviews 2005;6:108–122.
17. Gupta PK. Trends Biotechnol 2008;26:602–611. [PubMed: 18722683]
18. Brakmann S, Lobermann S. Angew Chem Int Ed Engl 2002;41:3215–3217. [PubMed: 12207394]
19. Foldes-Papp Z, Angerer B, Thyberg P, Hinz M, Wennmalm S, Ankenbauer W, Seliger H, Holmgren A, Rigler R. J Biotechnol 2001;86:203–224. [PubMed: 11257532]
20. Jett JH, Keller RA, Martin JC, Marrone BL, Moyzis RK, Ratliff RL, Seitzinger NK, Shera EB, Stewart CC. J Biomol Struct Dyn 1989;7:301–309. [PubMed: 2557861]
21. Beaucage SL, Caruthers MH. Tetrahedron Lett 1981;22:1859–1862.
22. Anderson JP, Angerer B, Loeb LA. Biotechniques 2005;38:257–264. [PubMed: 15727132]
23. Giller G, Tasara T, Angerer B, Muhlegger K, Amacker M, Winter H. Nucleic Acids Res 2003;31:2630–2635. [PubMed: 12736313]
24. Tasara T, Angerer B, Damond M, Winter H, Dorhofer S, Hubscher U, Amacker M. Nucleic Acids Res 2003;31:2636–2646. [PubMed: 12736314]

25. Jager S, Rasched G, Kornreich-Leshem H, Engeser M, Thum O, Famulok M. J Am Chem Soc 2005;127:15071–15082. [PubMed: 16248646]
26. Weisbrod SH, Marx A. Chem Commun 2008:5675–5685.
27. Kessler C, Holtke HJ, Seibl R, Burg J, Muhlegger K. Biological Chemistry Hoppe-Seyler 1990;371:917–927. [PubMed: 2076199]
28. Korlach J, Bibillo A, Wegener J, Peluso P, Pham TT, Park I, Clark S, Otto GA, Turner SW. Nucleosides Nucleotides Nucleic Acids 2008;27:1072–1083. [PubMed: 18711669]
29. Smolina IV, Cherny DI, Nietupski RM, Beals T, Smith JH, Lane DJ, Broude NE, Demidov VV. Anal Biochem 2005;347:152–155. [PubMed: 16243289]
30. Rist MJ, Marino JP. Curr Organ Chem 2002;6:775–793.
31. Flanagan WM, Wolf JJ, Olson P, Grant D, Lin KY, Wagner RW, Matteucci MD. Proc Natl Acad Sci U S A 1999;96:3513–3518. [PubMed: 10097067]
32. Lin KY, Jones RJ, Matteucci M. J Am Chem Soc 1995;117:3873–3874.
33. Engman KC, Sandin P, Osborne S, Brown T, Billeter M, Lincoln P, Norden B, Albinsson B, Wilhelmsson LM. Nucleic Acids Res 2004;32:5087–5095. [PubMed: 15452275]
34. Sandin P, Borjesson K, Li H, Martensson J, Brown T, Wilhelmsson LM, Albinsson B. Characterization and use of an unprecedentedly bright and structurally non-perturbing fluorescent DNA base analogue. Nucleic Acids Res 2008;36:157–167. [PubMed: 18003656]
35. Sandin P, Stengel G, Ljungdahl T, Borjesson K, Macao B, Wilhelmsson LM. Nucleic Acids Res 2009;37:3924–3933. [PubMed: 19401439]
36. Stengel G, Purse BW, Wilhelmsson LM, Urban M, Kuchta RD. Biochemistry 2009;48:7547–7555. [PubMed: 19580325]
37. Ludwig J. Acta Biochim Biophys Hung 1981;16:131–133.
38. Goodman MF, Creighton S, Bloom LB, Petruska J. Crit Rev Biochem Mol Biol 1993;28:83–126. [PubMed: 8485987]
39. O'Neill, MA.; Barton, JK. Topics in Current Chemistry. Vol. 236. Berlin: Springer; 2004. DNA-mediated charge transport chemistry and biology, Long-range charge transfer in DNA I; p. 67-115.

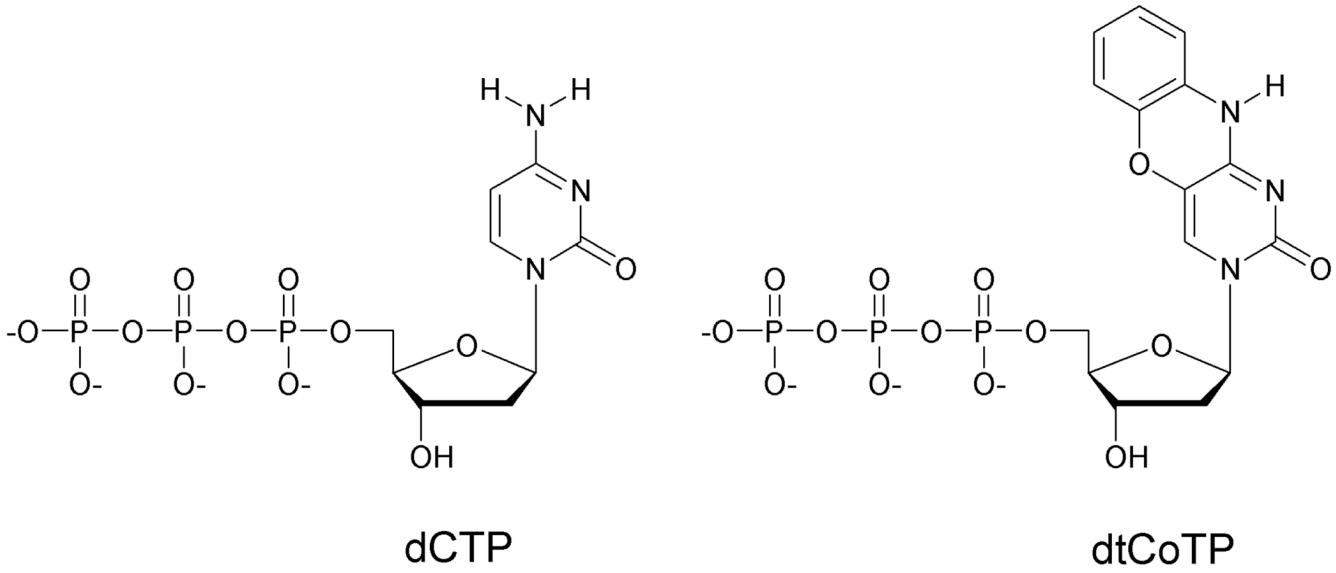

Figure 1.
Chemical structures of 2′-deoxycytidine 5′-triphosphate (CTP) and 1,3-diaza-2-oxo-phenoxazine-2’-deoxyribose-5’-triphosphate (dtCoTP).

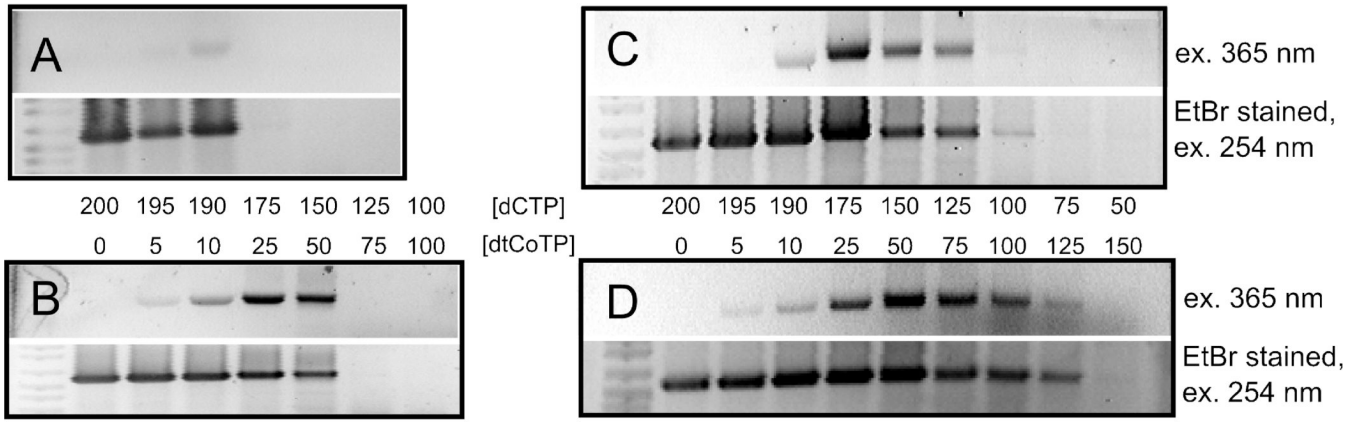

Figure 2.

Comparison between different DNA polymerases and different denaturation conditions. The PCR products obtained after 40 cycles were analyzed on 1.2 % agarose gels and the DNA bands were either visualized by excitation at 365 nm (top rows) or by staining with ethidium bromide (bottom rows). A) Taq pol. Denaturation at 95 °C/ 45 sec. B) Deep Vent pol. Denaturation at 95 °C/45 sec. C) Deep Vent pol. Denaturation at 99 °C/ 45 sec. D) Deep Vent pol. Denaturation in the presence of 15 % glycerol at 99 °C /45 sec.

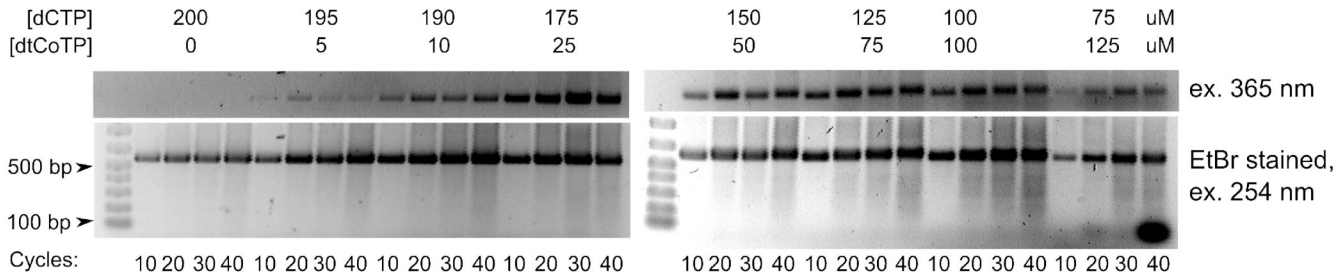

Figure 3.

PCR reactions catalyzed by Deep Vent pol at different mixing ratios of dCTP and dtCoTP. Reactions were performed using 10, 20, 30 or 40 amplification cycles. The top row displays the PCR fragments prior to staining with ethidium bromide; visualization is accomplished by exciting incorporated tCo at λ = 365 nm. All reactions were performed in the presence of 15 % glycerol, using denaturation at 99 °C/45 sec.

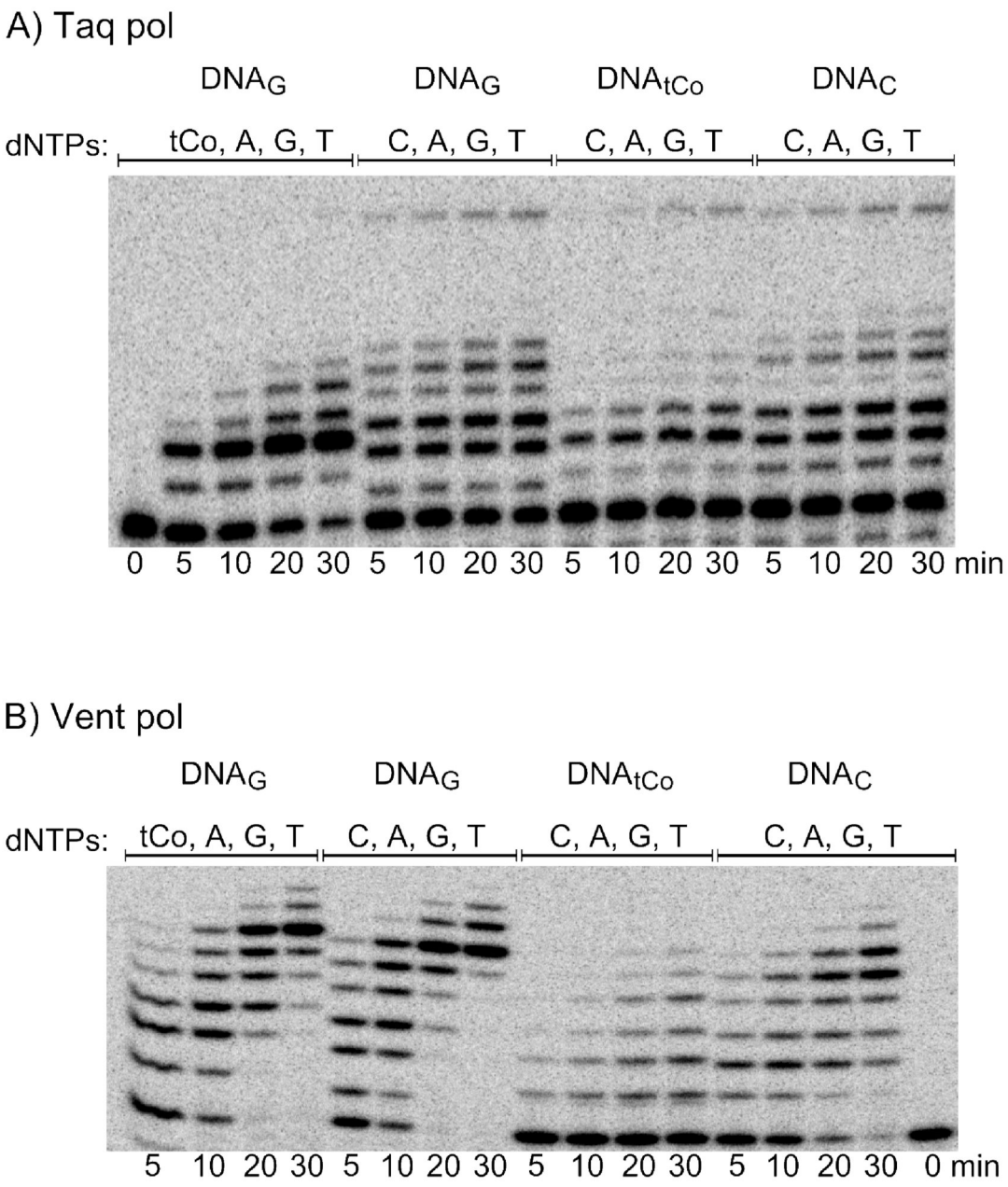

Figure 4.

Polymerization past tCo-G and G-tCo base pairs generated using Taq and Deep Vent pol and synthetic primer/templates (12 nt/25 nt long). First, 0.0125u/ul Taq (A) and 0.0005u/ul Deep Vent pol (B) were used to copy past a template G (DNA_G) either in the presence of dtCoTP, dGTP, dATP and dTTP or in the presence of all four natural nucleotides, respectively. Time points were withdrawn after 5, 10, 20 and 30 min. Second, time courses for primer polymerization past a template C (DNA_C) or a template tCo (DNA_{tCo}), respectively, in the presence of all for natural nucleotides were recorded. All reactions were performed at 37 °C.

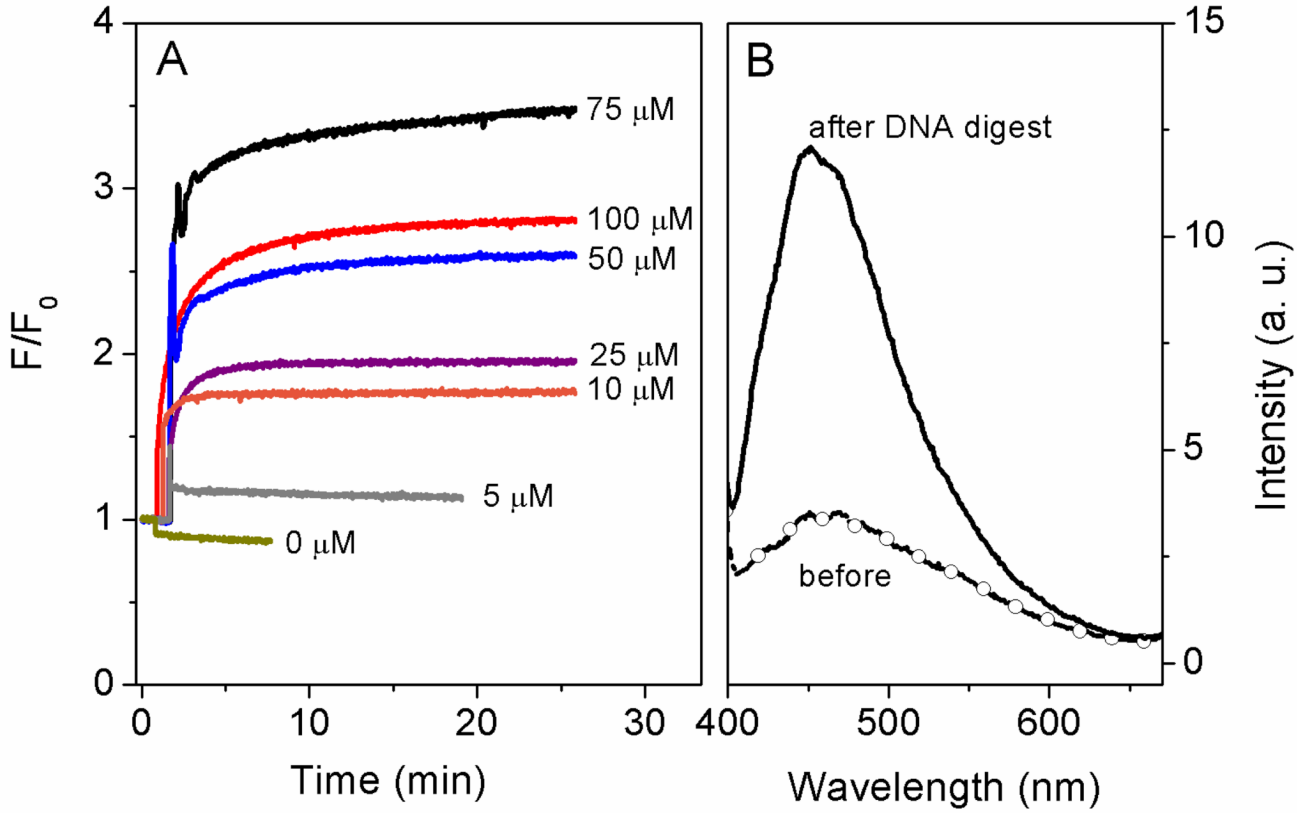

Figure 5.

Dequenching of tCo fluorescence upon enzymatic digestion of PCR products. PCR products were gel purified and treated with a mixture of DNAse I and Exonuclease I. A) Time course of fluorescence dequenching as DNA is broken down into tri-, di- and mononucleotides. F indicates the fluorescence intensity at a given time, F0 is the intensity measured before addition of the nucleases. PCR reactions were carried out using the dtCoTP concentration indicated in the figure, with [dCTP] + [dtCoTP] = 200 μM. B) Representative fluorescence spectra of the DNA fragment obtained with 75 μM dtCoTP before (white circles) and after treatment with the enzyme cocktail (black line).

Table 1

Relative catalytic efficiency for the incorporation of dtCoTP across G and A

dNTP in competition with dtCoTP	Templating base	*Relative catalytic efficiency $\left(\frac{k_{cat}}{K_M}\right)_{dtCoTP}\left(\frac{k_{cat}}{K_M}\right)_{dNTP}$	
		Deep Vent pol	Taq pol
dCTP	G	1.5	7.7
dTTP	A	0.1	0.3

$$\frac{1}{{}^{*}\text{fraction}_{dNTP}} = \frac{\left(\frac{kcat}{K_M}\right)_{dtCoTP}}{\left(\frac{kcat}{K_M}\right)_{dNTP}} \cdot \frac{[dtCoTP]}{[dNTP]}$$

Table 2

Kinetic parameters for the insertion of natural dNTPs across from tCo.

dNTP	DNA_N	V_{max} (SD) $\left[\frac{\%\ extension}{min}\right]$	K_M (SD) [μM]	V_{max}/K_M $\left[\frac{\%\ extension}{\mu M \cdot min}\right]$	Discrimination*
Deep Vent pol					
dGTP	DNA_C	11.4 (0.4)	0.29 (0.05)	39	1
dGTP	DNA_{tC}	3.7 (0.1)	1.7 (0.3)	2.2	18
dATP	DNA_{tC}	3.8 (0.1)	44 (15)	0.09	440
Taq pol					
dGTP	DNA_C	33 (1)	0.43 (0.07)	77	1
dGTP	DNA_{tC}	10 (1)	12 (3)	0.8	96
dATP	DNA_{tC}	0.58 (0.03)	20 (4)	0.03	2600

* Discrimination is defined as V_{max}/K_M for the incorporation of dGTP into DNA_C, divided by V_{max}/K_M for the incorporation of a given dNTP into DNA_{tCo}.

Table 3

Efficiency of polymerization past tCo-G and G-tCo base pairs.

dNTP's	Template	Total primer extension (%)	Primer extended past primer + 2 position (%)
		Deep Vent pol	
tCo, A, G, T	G	88	63
C, A, G, T	G	89	82
C, A, G, T	tCo	20	24
C, A, G, T	C	64	53
		Taq pol	
tCo, A, G, T	G	59	14
C, A, G, T	G	53	62
C, A, G, T	tCo	26	33
C, A, G, T	C	39	49

Table 4

Quantum yields of tCo-containing oligonucleotides.

DNA sequence, X = tCo	Quantum Yield [a] (SD)
5′-TGT**X**A**X**CAACAACTGT	0.25 (0.04)
5′-TGT**X**AC**X**AACAACTGT	0.30 (0.03)
5′-TGT**X**ACCAA**X**AACTGT	0.20 (0.03)
5′-TGT**X**ACCAACAA**X**TGT	0.27 (0.01)
5′-TGT**X**A**X**CAACAACTGT 3′-ACAGTGGTTGTTGACA	0.20 (0.02)
5′-TGT**X**AC**X**AACAACTGT 3′-ACAGTGGTTGTTGACA	0.15 (0.03)
5′-TGT**X**ACCAA**X**AACTGT 3′-ACAGTGGTTGTTGACA	0.15 (0.02)
5′-TGT**X**ACCAACAA**X**TGT 3′-ACAGTGGTTGTTGACA	0.16 (0.02)
5′-TCTACTATA**XXXX**ATGTGATATGGA	0.03 (0.004)
5′-TCTACTATTCTA**X**ATGTGATATGGA	0.30 (0.04)
d**X**TP	0.30 (0.04)

[a] The quantum yield standard was quinine sulfate in 0.1 M H_2SO_4 (QY = 0.55). Measurements were performed in 0.5 × phosphate buffered saline at room temperature and the data show the average of three independent measurements.